Foraging plasticity diversifies mercury exposure sources and bioaccumulation patterns in the world's largest predatory fish

Gaël Le Croizier, Jeroen Sonke, Anne Lorrain, Marina Renedo, Mauricio Hoyos-Padilla, Omar Santana-Morales, Lauren Meyer, Charlie Huveneers, Paul Butcher, Felipe Amezcua-Martinez, et al.

Journal of Hazardous Materials
March 2022, Volume 425, Pages 127956 (9p.)
https://doi.org/10.1016/j.jhazmat.2021.127956
https://archimer.ifremer.fr/doc/00738/85003/

Foraging plasticity diversifies mercury exposure sources and bioaccumulation patterns in the world's largest predatory fish

Le Croizier Gaël [1, 2, *], Sonke Jeroen E [1], Lorrain Anne [3], Renedo Marina [1], Hoyos-Padilla Mauricio [4, 5], Santana-Morales Omar [6], Meyer Lauren [7, 8], Huveneers Charlie [7], Butcher Paul [9], Amezcua-Martinez Felipe [2], Point David [1]

[1] UMR Géosciences Environnement Toulouse (GET), Observatoire Midi Pyrénées (OMP), 14 avenue Edouard Belin, 31400 Toulouse, France
[2] Instituto de Ciencias del Mar y Limnología, Universidad Nacional Autónoma de México. Av. Joel Montes Camarena S/N. Mazatlán, Sin. México, 82040
[3] Univ Brest, CNRS, IRD, Ifremer, LEMAR, F-29280 Plouzané, France
[4] Pelagios-Kakunjá A.C. Sinaloa 1540. Col. Las Garzas. C.P. 23070. La Paz, B.C.S., México
[5] Fins Attached: Marine Research and Conservation 19675 Still Glen Drive Colorado Springs, CO 80908, USA
[6] ECOCIMATI A.C., 22800, Ensenada, Baja California, Mexico
[7] Southern Shark Ecology Group, College of Science and Engineering, Flinders University, Adelaide, SA 5042, Australia
[8] Georgia Aquarium, Atlanta, GA, 30313, USA
[9] NSW Department of Primary Industries, National Marine Science Centre, Coffs Harbour, NSW 2450, Australia

* Corresponding author : Gaël Le Croizier, email address : gael.lecroizier@hotmail.fr

Abstract :

Large marine predators exhibit high concentrations of mercury (Hg) as neurotoxic methylmercury, and the potential impacts of global change on Hg contamination in these species remain highly debated. Current contaminant model predictions do not account for intraspecific variability in Hg exposure and may fail to reflect the diversity of future Hg levels among conspecific populations or individuals, especially for top predators displaying a wide range of ecological traits. Here, we used Hg isotopic compositions to show that Hg exposure sources varied significantly between and within three populations of white sharks (Carcharodon carcharias) with contrasting ecology: the north-eastern Pacific, eastern Australasian, and south-western Australasian populations. Through Δ200Hg signatures in shark tissues, we found that atmospheric Hg deposition pathways to the marine environment differed between coastal and offshore habitats. Discrepancies in δ202Hg and Δ199Hg signatures among white sharks provided evidence for intraspecific exposure to distinct sources of marine methylmercury, attributed to population and ontogenetic shifts in foraging habitat and prey composition. We finally observed a strong divergence in Hg accumulation rates between populations, leading to three times higher Hg concentrations in large Australasian sharks compared to north-eastern Pacific sharks, and likely due to different trophic strategies adopted by adult sharks across populations. This study illustrates the variety of Hg exposure sources and

bioaccumulation patterns that can be found within a single species and suggests that intraspecific variability needs to be considered when assessing future trajectories of Hg levels in marine predators.

Graphical abstract

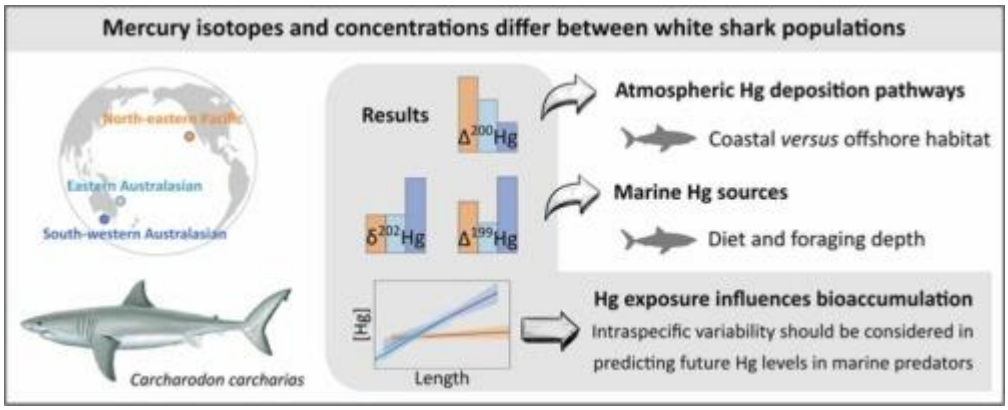

Highlights

► Mercury (Hg) isotopes were analyzed in three white shark populations ► $\Delta^{200}Hg$ values showed different atmospheric Hg deposition pathways across habitats ► $\Delta^{199}Hg$ and $\delta^{202}Hg$ values indicated population variations in marine Hg exposure ► Hg concentrations in adult sharks differed by a factor of three between populations ► Hg contamination in ocean predators may not vary uniformly under global change

INTRODUCTION

The Anthropocene era has led to the global decline of shark populations, due to overfishing, bycatch, and other indirect threats including habitat loss and changes in prey availability [1–4]. Removing predators can result in trophic cascading effects impairing the structure and functioning of marine ecosystems [5–7]. In this context, it has recently been suggested that the white shark (*Carcharodon carcharias*), the world's largest predatory fish, may become extinct during the 21st century, along with its ecosystem role as apex predator [7]. Despite a global decline in abundance over the past half century, the different populations of white sharks do not follow the same trajectories [8]. While some populations are considered stable, including in eastern Australasia [9], a decrease in the abundance of white sharks has been observed in other regions, such as the Mediterranean sea [10].

White sharks are highly mobile, generalist predators with foraging plasticity encompassing a wide range of prey and habitats [11]. In the north-eastern Pacific (NEP), white sharks perform seasonal migrations from inshore seal colonies to offshore areas where they likely forage on deep mesopelagic prey [12,13]. In Australian waters, white sharks are divided into two populations, namely the eastern Australasian (EA) and south-western Australasian (SWA) populations [14]. In the SWA population, although occasional offshore movements were observed, immature and adult sharks mainly occupy coastal waters on the continental shelf where they primarily target locally abundant pinnipeds [15–17]. Conversely, EA sharks show an ontogenetic (developmental) shift in habitat use, with immature sharks being mainly restricted to coastal waters [18,19] and larger individuals performing wide-spread movements across ocean basins to New Zealand and tropical Pacific islands [20,21]. As the east coast of Australia is devoid of primary seal colonies, coastal fish are the predominant prey for immature EA sharks [22].

Mercury (Hg) is a global pollutant of particular concern to human and wildlife health. Mercury is emitted to the atmosphere from natural and anthropogenic sources and largely deposited to the ocean surface, where a fraction is converted to methylmercury (MeHg) by microorganisms [23]. Methylmercury is characterized by strong neurotoxicity, bioaccumulation in marine biota and unique biomagnification properties in food webs [24]. Due to their longevity and high trophic level, white sharks are among the marine species displaying the highest concentrations of Hg, assumed to be predominantly MeHg [12,25]. The impact of Hg exposure on shark neurophysiology is still poorly understood [26,27] and shark species could exhibit metabolic mechanisms allowing them to reduce toxicity, such as *in vivo* demethylation of MeHg [28]. However, the particularly high Hg concentrations found in white sharks likely induce deleterious effects (e.g. damage to the central nervous system, loss of neurons, sensory and motor deficits, oxidative stress) as observed in marine mammals and other shark species [27,29,30] and represent an additional pressure on this vulnerable species.

In the context of global change, the future trend of Hg concentrations in marine predators remains uncertain. Empirical studies do not reach consensus, as a decrease [31,32], stability [33,34] or increase [35–37] in predator Hg content has been observed over the past decades, depending on the species and regions considered. Most model projections predict increased Hg levels in meso and top predators under different scenarios of seawater warming and dietary changes due to overfishing of prey stocks [38–40]. However, current predictions ignore the foraging plasticity and wide range of ecological traits of apex predators such as white sharks. This could mask the heterogeneity in future contamination patterns within a single species, as individual foraging strategies have been shown to influence Hg exposure and ultimately Hg levels in mesopredators [41]. It is therefore essential

to characterize and understand intraspecific variability in Hg exposure to better predict the effects of global change on predator contamination and marine ecosystem health.

In recent years, the measurement of the natural abundances of Hg stable isotopes has greatly improved knowledge on the sources of exposure, transfer pathways, and metabolism of Hg in marine consumers [42–44]. Many abiotic (e.g. photoreduction, volatilization) [45,46] and biotic processes (e.g. methylation, demethylation) [28,47,48] result in mass-dependent isotope fractionation (MDF, reported as δ^{202}Hg), whereas mass-independent fractionation of odd-mass number isotopes (odd-MIF, reported as Δ^{199}Hg or Δ^{201}Hg) has been primarily observed during aquatic photochemical reactions [45]. In addition, significant MIF of even-mass number isotopes (even-MIF, reported as Δ^{200}Hg) is thought to occur via Hg photochemistry in the upper atmosphere [49]. The analysis of Hg isotopes in marine biota therefore provides information about atmospheric Hg deposition pathways to the marine environment [50], Hg methylation / demethylation processes in the water column and sediments [51], as well as on species biology and ecology, such as Hg metabolism and foraging habitat [12,52]. Mercury isotopes have been successfully used to distinguish Hg exposure between sedentary, low trophic level marine fish populations [53,54]. However, uncertainty remains regarding the possibility of applying this method to assess intraspecific variability in Hg exposure in highly mobile top predators such as white sharks.

To evaluate intraspecific variability in Hg contamination in marine apex predators, we tested the capability of Hg isotopes to identify differences in Hg exposure among three white shark populations (NEP, SWA, and EA) with contrasting ecology and large spatial scales. We discussed the potential links between Hg sources and the known ecological characteristics of these populations. We also sought to describe the dynamics of Hg bioaccumulation within each population. We hypothesized that Hg exposure and levels may vary between

populations, making the assessment of Hg fate in marine predators under global change more complex than previously thought.

MATERIALS AND METHODS

Sample collection

- North-eastern Pacific population

White sharks (n = 30) were sampled at Guadalupe Island (Mexico) between September and November in 2016, 2017 and 2018 (Figure 1). Free-swimming white sharks were attracted with bait near the research vessel. Muscle samples were taken using a biopsy probe targeting the tissue directly below the dorsal fin. After collection, samples were immediately transferred to a -20 °C freezer onboard the vessel.

- South-western Australasian population

White shark samples (n = 40) were collected from January 2015 to July 2020 at the Neptune Islands Group Marine Park, South Australia (Figure 1), where free-swimming sharks were targeted opportunistically throughout the year during standard cage-diving operations. Sharks were attracted to the cage-diving vessels using a combination of attractants. Biopsies were taken from diving cages or from the surface using a single 20-mm rubber speargun, with the end of the 1.3 m spear modified into a hollow 1 cm diameter stainless steel biopsy probe [55], targeting the dorsal or upper flank musculature directly below the dorsal fin. Biopsies were immediately frozen (−4 °C) and transported to the laboratory where white muscle tissue was dissected from the sub-dermal tissue and skin.

- Eastern Australasian population

White sharks (n = 44) were sampled along the east coast of New South Wales, Australia (within a radius of ~30 km around the town of Ballina, Figure 1) between 2016 and 2020, using SMART drumlines as part of a bather protection research program [56,57]. After capture, sharks were secured to the side of the vessel and a muscle sample was taken using an 0.8 cm sterile biopsy punch (Kai medical) targeting the tissue directly behind the dorsal fin. Tissue samples were immediately placed into a 5 ml screw cap vial on ice and transferred to a -4 °C freezer.

Individual sharks from all three populations (NEP, SWA, and EA) were sexed (based on clasper presence/absence), and total length was measured to the nearest 10 cm using visual size estimates (NEP and SWA) [58] or to the nearest 1 cm using a certified tape (EA) [56,57].

Mercury concentration analysis

Once in the laboratory, muscle samples were lyophilized and homogenized using an electric grinder that was rinsed with alcohol between samples (Figure S1). Total Hg (THg) concentration was determined on aliquots (around 10 mg) of homogenized samples by combustion, gold trapping and atomic absorption spectrophotometry using a DMA80 analyzer (Milestone, USA). As THg is predominantly in the MeHg form in shark muscle [28,59–63], THg was used as a proxy for MeHg concentration, in accordance with previous studies [12,64]. Total Hg concentrations in samples are expressed on a dry weight basis ($ng \cdot g^{-1}$ dw). Only one analysis was performed per sample, but the accuracy and reproducibility of the method were established using two freeze-dried certified biological material: a tuna fish flesh homogenate reference material (IAEA 436, IRMM) and a lobster hepatopancreas reference material (TORT 3, NRCC). The certified values for IAEA 436 (4.19 ± 0.36 $\mu g \cdot g^{-1}$ dw, n = 10) were reproduced (measured value: 4.33 ± 0.19 $\mu g \cdot g^{-1}$ dw) within the confidence limits. The

certified values for TORT 3 (0.292 ± 0.022 $\mu g \cdot g^{-1}$ dw) were also reproduced (measured value: 0.286 ± 0.024 $\mu g \cdot g^{-1}$ dw, n = 10) within the confidence limits. The detection limit was 0.005 $\mu g \cdot g^{-1}$ dw.

Mercury isotope analysis

Aliquots of approximately 10 mg of dry muscle were left over night (~12 hours) at ambient room temperature in 3 mL of concentrated bi-distilled nitric acid (HNO_3). A volume of 1 mL of hydrogen peroxide (H_2O_2) was added, and samples were digested on a hotplate for 6h at 100°C. A volume of 100 µL of BrCl was then added to ensure a full conversion of MeHg to inorganic Hg. The digest mixtures were finally diluted in inverse aqua regia (3 HNO_3: 1 HCl, 20 vol.% MilliQ water) to reach a nominal Hg concentration of 1 $ng \cdot g^{-1}$. Certified reference materials (ERM-BCR-464) and blanks were prepared in the same way as tissue samples. Mercury isotope composition was measured by multi-collector inductively coupled plasma mass spectrometry (MC–ICP–MS, Thermo Finnigan Neptune Plus) with continuous-flow cold vapor (CV) generation using Sn (II) reduction (CETAC HGX-200). Mercury isotope ratios are expressed in δ notation and reported in parts per thousand (‰) deviation from the NIST SRM 3133 standard, following sample-standard bracketing according to the following equation: $\delta^{XXX}Hg$ (‰) = [$(^{XXX}Hg/^{198}Hg)_{sample}$ / $(^{XXX}Hg/^{198}Hg)_{NIST\ 3133}$) -1] X 1000 where xxx represents the mass of each mercury isotope. $\delta^{202}Hg$ represents Hg MDF, and Δ notation is used to express Hg MIF by the following equation:

$\Delta^{xxx}Hg$ (‰) = $\delta^{xxx}Hg$ – ($\delta^{202}Hg$ X a)

where a = 0.2520, 0.5024 and 0.7520 for isotopes 199, 200 and 201, respectively.

Total Hg in the diluted solutions was quantified by MC-ICP-MS using ^{202}Hg signals: mean recoveries of 98 ± 11% (n = 84) for samples and 96 ± 6 and dilution% (n = 12) for certified reference materials were found. Mercury levels in blanks were below the detection limit of 0.005 ng·g^{-1}. Reproducibility of Hg isotope measurements was assessed by analyzing UM-Almadén (n = 24), ETH-Fluka (n = 22) and the biological tissue procedural standard ERM-BCR-464 (n = 12) (Table S1). Measured isotope signatures as well as analytical reproducibility of standards (UM-Almadén, ETH-Fluka and ERM-BCR-464) were found to be in agreement with previously published values [42,65,66] (Table S1). Duplicate analysis was performed on a subset of 15 white shark tissues to assess the analytical uncertainty of δ^{202}Hg (2SD = 0.12‰) and Δ^{199}Hg values (2SD = 0.10 ‰) in the samples.

Data analysis

For comparison of Hg isotope signatures among white shark populations, data were first checked for normality (Shapiro–Wilk tests) and homogeneity of variances (Bartlett tests). One-way analyses of variance (ANOVAs) were applied when these conditions were met, followed by Tukey's HSD tests. In the absence of homoscedasticity, Welch's ANOVAs with Games-Howell post-hoc tests were used. Linear regressions were used to assess relationships between different Hg isotope values, between Hg concentration and shark length, or between Hg isotope values and shark length. Analyses of covariance (ANCOVAs) were used to compare Hg accumulation rates between populations. Generalized linear models (GLMs) were used to evaluate the influence of population, shark length, gender, and Hg isotope values (Δ^{200}Hg, Δ^{199}Hg and δ^{202}Hg) on Hg levels. Based on the analysis of the residuals, a Gaussian distribution and identity link function were used in the GLMs. The models were built using backward stepwise selection, ranked based on Akaïke's Information

Criteria adjusted for small sample sizes (AIC_c) and compared using ΔAIC_c and Akaike weights (w_i). All statistical analyses were performed using the open source software R (4.1.1 version).

RESULTS AND DISCUSSION

Atmospheric Hg deposition pathways

White shark Δ^{200}Hg values were close to zero in all three populations (Table 1). The Δ^{200}Hg signature has previously been used as a conservative tracer of atmospheric inorganic Hg deposition pathways [67,68]. The deposited Hg subsequently becomes the substrate for MeHg production in marine environments. Δ^{200}Hg mainly discriminates between dissolution of gaseous Hg(0) (slightly negative Δ^{200}Hg of -0.05 ‰) and wet and dry deposition of inorganic Hg(II) through precipitation and dry deposition (positive Δ^{200}Hg values of 0.14 ‰) [69]. Terrestrial plants and soils have been shown to take up atmospheric Hg(0), and continental runoff by rivers to the oceans thus constitutes an additional Hg source with Δ^{200}Hg similar to Hg(0) [70]. As coastal food webs receive Hg from all three sources, their Δ^{200}Hg values are generally closer to the Hg(0) than the Hg(II) end-member [68,71]. Conversely, pelagic ecosystems show equal contributions of Hg(0) and Hg(II) deposition, resulting in Δ^{200}Hg signatures around 0.05 ‰ [67,72]. Here, the mean Δ^{200}Hg values of 0.06, 0.04, and 0.03 ‰ for NEP, EA and SWA populations respectively (Table 1) would thus reflect an equivalent contribution of Hg(0) and Hg(II) sources, characteristic of pelagic environments [50]. However, the NEP population displayed a significantly higher Δ^{200}Hg than the SWA population ($p < 0.05$, Figure 2A), with EA sharks showing intermediate values. Despite the small magnitude of even-MIF, Δ^{200}Hg values revealed a greater contribution of Hg(II) inputs in the NEP population compared to SWA sharks. This hypothesis agrees with a previous study showing

that NEP white sharks were dietary exposed to mesopelagic MeHg [73], which is mainly produced from Hg(II) supplied by precipitation and dry deposition in the subtropical Pacific [72]. Although Hg isotope signatures of prey have not yet been characterized for Australasian sharks, movement data showed that SWA sharks primarily occupy coastal waters [15,16] (Table 1), which are believed to receive more Hg(0) inputs via continental runoff. The coastal affinity of SWA sharks, opposed to the pelagic foraging behavior of NEP sharks, could thus explain the variations in Δ^{200}Hg observed between these populations (i.e. higher Δ^{200}Hg in NEP sharks, Figure 2A).

A recent global analysis of marine Δ^{200}Hg (including particulate Hg, sediments, and biota) showed the occurrence of a latitudinal isotopic gradient, with lower Δ^{200}Hg values at high latitudes, indicating larger ocean Hg(0) uptake compared to intermediate and tropical areas [50]. However, this study reported similar Δ^{200}Hg values at the latitudes corresponding to our sampling sites, i.e., around 30°N and 30°S (Figure 1). The variability in Δ^{200}Hg observed in our study seems to be governed by differences in atmospheric Hg sources between coastal and offshore shark habitats, rather than by a latitudinal gradient in Δ^{200}Hg at the global scale.

Marine MeHg sources

Mercury odd-MIF signatures in marine biota are not affected by trophic transfers or metabolic processes [47,74] and are specifically derived from the photodegradation of MeHg in seawater prior to food web biomagnification [42]. Although similar Δ^{201}Hg/Δ^{199}Hg ratios across regions suggest a common mechanism for MeHg photodegradation (Figure S2 and additional discussion), we found significant variations in Δ^{199}Hg values between populations ($p < 0.01$, Figure 2B), indicating exposure to distinct MeHg pools that experienced different intensities

of photodegradation. In the open ocean or near offshore islands, where marine organisms are mainly exposed to pelagic MeHg, fish species are characterized by Δ^{199}Hg values generally higher than 1 ‰ [28,42,75]. Conversely, marine fishes exposed to MeHg produced in coastal sediments or turbid waters, where light penetration is limited, display significantly lower Δ^{199}Hg values (typically lying between 0 and 1 ‰) [71,76,77]. In addition, as Hg photodegradation decreases with light attenuation in the water column, Δ^{199}Hg values generally decrease with increasing foraging depth in marine fishes [42,52,75]. Δ^{199}Hg values in a marine predator may thus reflect vertical or horizontal habitat use, or a combination of both, depending on the environment considered [78]. As it was previously shown that NEP sharks are primarily exposed to deep and offshore MeHg [73], and SWA and EA sharks occupy mainly coastal and shallow habitats [15,16,18,19], Δ^{199}Hg signatures were expected to differ between NEP and Australasian populations, as observed in our dataset (Figure 2B). Surprisingly, the NEP population showed a Δ^{199}Hg of 1.54 ‰, which fell between the Δ^{199}Hg of SWA and EA populations (1.69 and 1.25 ‰, respectively) (Table 1). Photochemical degradation of MeHg is known to vary globally, primarily related to water clarity and UV penetration depth [79]. Differences in habitat characteristics and water clarity (based on Secchi depth; Table 1) therefore suggest variations in Δ^{199}Hg baselines across distant regions, complicating direct comparison of NEP and Australasian populations. By focusing on spatially close populations, a gap in Δ^{199}Hg values was also observed between SWA and EA sharks, despite an apparent similarity in vertical and horizontal habitat use for the size classes considered [15,16,18,19], and in average water clarity in both regions [80] (Table 1). However, when closely examining the fine-scale distribution in the water column, SWA sharks were observed to primarily occupy the upper 50 m [15], while EA sharks were most abundant between 50 and 130 m depth [81]. As the MeHg photodegradation gradient is steep in shallow depths [42,73], this

inconspicuous but significant difference in vertical habitat is consistent with the Δ^{199}Hg variation observed between Australasian (SWA and EA) populations. This exemplifies the ability and sensitivity of the Δ^{199}Hg tracer to capture slight variations in vertical habitat used by nearby predator populations.

Although many biotic and abiotic processes affect Hg MDF, hepatic MeHg demethylation has been identified as one of the major mechanisms leading to increased δ^{202}Hg values in the muscle tissue of predators such as marine mammals [44,47], seabirds [82,83], and more recently sharks [28,64]. The preferential demethylation of light Hg isotopes in the liver increases δ^{202}Hg in the remaining MeHg pool, with a fraction ultimately stored in muscle [47,82]. Here, we found high δ^{202}Hg values (up to 1.43 ‰ in the SWA population; Table 1) and near zero Δ^{199}Hg/δ^{202}Hg slopes (Figure S3 and additional discussion) which may suggest substantial MeHg demethylation in white sharks, as previously established for other large species such as bull and tiger sharks [52]. Alternatively, it may result from the consumption of marine mammals, which can represent an important part of the white shark diet [22,84] and which also display elevated δ^{202}Hg values due to MeHg demethylation [47,85]. The higher δ^{202}Hg found in SWA sharks compared to the NEP and EA populations (Figure 2) could thus be the result of either higher demethylation or more frequent consumption of marine mammals. In our study, SWA sharks had much higher Hg concentrations than NEP sharks (Table 1), which does not support the hypothesis of higher demethylation. However, the second hypothesis is supported by the modest contribution of mammals to Hg exposure of NEP sharks [73] and dietary intake of immature EA sharks [22], while the SWA shark samples were collected near a large colony of pinnipeds (Neptune Islands Group Marine Park; Figure 1).

Individual variability in Hg exposure

No variation in Hg isotope signatures related to gender or body length has been previously found in NEP sharks, suggesting a common Hg exposure at the population scale [73]. Conversely, ontogenetic variability was observed here within the two Australasian populations. In the EA population, Δ^{199}Hg was positively correlated with shark total length (Figure 3A). Previous studies of the EA white shark population have shown an ontogenetic increase in travelling behavior [81], with coastal areas dominated by small immature individuals [18,19,22,86] and large sharks more likely to undertake large-scale offshore migrations [20,21,87]. Such an increase in offshore dispersal would result in greater exposure to pelagic MeHg sources, typically characterized by higher Δ^{199}Hg values [28,42,75] than MeHg produced in coastal habitats [71,76,77], and would explain the ontogenetic variation in Δ^{199}Hg found in EA sharks.

In SWA sharks, both δ^{202}Hg and Δ^{200}Hg were found to increase with size (Figure 3B, 3C). Mercury metabolism in sharks is supposed to increase δ^{202}Hg values over time, through enhanced MeHg demethylation in older individuals [52]. In addition, white sharks are known to increase their consumption of marine mammals as they grow larger [84], which may increase the uptake of MeHg with δ^{202}Hg higher values [73]. It is therefore difficult to deconvolute the different mechanisms (Hg metabolism, change in prey) responsible for ontogenetic variations in the δ^{202}Hg signature. However, as δ^{202}Hg values did not increased with size in NEP and EA populations, changes in δ^{202}Hg are unlikely to be caused by metabolism alone. Considering that oceanic Δ^{200}Hg baselines are generally slightly higher than coastal baselines [67,71,72], the higher Δ^{200}Hg observed in large SWA sharks suggests an ontogenetic increase in offshore movements in this population. This is consistent with a recent tracking study documenting movements of large SWA sharks (> 4.5 m) off the continental shelf and

suggesting that females may disperse further offshore than males [15]. While we did not observe differences in Hg exposure between sexes, Δ^{200}Hg values provide evidence for an ontogenetic change in foraging habitat in the SWA population.

Mercury bioaccumulation

Log-transformed THg concentrations were positively correlated with shark length (a proxy for age) in Australasian sharks (Figure 4) and the log(THg)/length slopes were similar in SWA and EA populations (ANCOVA, $p > 0.05$). These results indicate a comparable rate of Hg bioaccumulation in the two Australasian populations. Methylmercury bioaccumulation in fish muscle results from a high MeHg assimilation efficiency, strong binding to cysteine residues of proteins and low excretion rate [88,89]. Moreover, MeHg stored in muscle comes from the residual blood MeHg exiting from the liver after *in vivo* demethylation. As MeHg is the dominant form of Hg in shark muscle [52,59,61], increased Hg concentration in the muscle of Australasian sharks may imply that trophic exposure to MeHg exceeds demethylation capacity. Our findings are consistent with a previous study which observed an increase in Hg concentration with size in juvenile EA individuals [90]. In contrast, no increase in Hg concentration with age was observed in NEP sharks (Figure 4), suggesting a balance between MeHg exposure and demethylation/excretion. Consequently, while Hg concentrations were similar in all three populations for smaller sharks (i.e., 11 and 12 ppm at 2.5 m total length for Australasian and NEP sharks, respectively), Australasian populations were three times more contaminated than the NEP population for larger sharks (e.g., 30 *versus* 10 ppm at 4.5 m total length for SWA and NEP sharks, respectively; Figure S4).

Similar muscle Hg concentrations observed in young white sharks do not argue for variations in marine MeHg baselines across regions. However, the difference in Hg

accumulation kinetics found between Australasian and NEP populations (Figure 4) could be related to different trophic strategies adopted by adult sharks. While δ^{202}Hg values suggest a size-based increase in MeHg uptake from marine mammals consumption in SWA sharks (Figure 3B), the NEP population is thought to be primarily exposed to MeHg from mesopelagic prey with limited contribution from pinnipeds, regardless of size [73]. As predators, marine mammals generally display higher Hg content than mid-trophic mesopelagic species [91,92]. A greater proportion of mammals in the diet of adult SWA sharks could thus partly explain their higher δ^{202}Hg values and Hg concentrations compared to the NEP population. This assumption is consistent with the outputs of generalized linear models used to predict Hg levels in white shark muscle. The top-ranked model (w_i = 0.60) included δ^{202}Hg, length and population, and δ^{202}Hg was the best stand-alone predictor of Hg concentration, explaining 36% of Hg variation in shark muscle (Table S2). This result revealed that consumption of marine mammals (exhibiting high δ^{202}Hg values [73]) could be a major driver of Hg levels in white sharks. In the future, this hypothesis can be verified by comparing the trophic level of adult sharks from the NEP and Australasian populations, but may require the use of amino acid nitrogen isotopic analysis to overcome spatial variations in isotopic baselines [93].

CONCLUSION

Global change is expected to influence Hg contamination in marine biota, yet intra-species differences in Hg exposure are rarely considered. Here, we applied for the first time the recent technique of Hg isotope analysis to characterize dietary Hg exposure across different populations of white sharks, the world's largest predatory fish. Our results revealed that the broad ecological spectrum of white sharks implies exposure to different sources of

Hg among individuals, likely leading to the marked differences in Hg bioaccumulation patterns observed between populations. Given this large intraspecific variability, predicting Hg levels in marine predators under global change could be more complex than previously thought. Future modelling research should therefore focus on a widely distributed top predator model species and account for population variations in Hg exposure and concentration to improve projections of predator Hg levels at the global scale.

Acknowledgments

Gaël Le Croizier was supported by a postdoctoral grant from the French National Research Institute for Sustainable Development (IRD) and the ISblue "Interdisciplinary graduate School for the blue planet" project (ANR-17-EURE-0015). We thank the French National Research Agency ANR-17-CE34-0010 project 'Unraveling the origin of methylMERcury TOXin in marine ecosystems' (MERTOX, PI DP) for providing financial support for Hg isotope analysis. The project was funded in Mexico by Alianza WWF-TELCEL, The Annemberg Foundation, International Community Foundation, Fins Attached Marine Research and Conservation and Pfleger Institute of Environmental Research. Field work in Mexico was greatly facilitated through courtesies extended to us by personnel of the University of California, Davis, Centro Interdisciplinario de Ciencias Marinas (CICIMAR), Secretaría de Marina, Comisión de Areas naturals Protegidas (CONANP), Island Conservation (GECI), Horizon Charters, Islander Charters, Solmar V, Club Cantamar and local fishermen from Guadalupe Island. In Mexico, white shark samples were collected under permits from the Secretaría del Medio Ambiente y Recursos Naturales (SEMARNAT): OFICIO NUM.SGPA/DGVS/07052/16 in 2016, OFICIO

NUM.SGPA/DGVS/06673/17 in 2017 and OFICIO NUM.SGPA/DGVS/004284/18 in 2018. Fieldwork in South Australia was possible thanks to the logistic support of the white shark cage-diving industry. We also thank the Save Our Seas Foundation, Holsworth Wildlife Research Endowment (HWRE2016R2098), Oceania Chondrichthyan Society and Passions of Paradise for providing funding to support sample collection. In South Australia, samples were collected in accordance with DEWNR permit #Q26292 and Flinders University Animal Ethics Committee approval #398 for South Australian samples. In New South Wales (NSW), samples were collected by the NSW DPI shark research team and SMART drumline contractors. NSW samples were collected under NSW DPI 'scientific' (Ref. P01/0059(A)), 'Marine Parks' (Ref. P16/0145-1.1) and 'Animal Care and Ethics' (ACEC Ref. 07/08) permits as part of the Shark Management Strategy. We also thank Jonathan Werry for his contribution to shark sampling in Eastern Australia. White shark samples were exported from Mexico under the CITES permit (number MX007) of the Universidad Nacional Autónoma de México and from Australia under the CITES permit (number AU089) of Flinders University. Samples were imported in France under the CITES permit (number FR75A) of the Muséum National d'Histoire Naturelle. We thank Laure Laffont and Jérôme Chmeleff for expert management of the OMP mercury and mass spectrometry facilities.

References

(1) Baum, J. K.; Myers, R. A.; Kehler, D. G.; Worm, B.; Harley, S. J.; Doherty, P. A. Collapse and Conservation of Shark Populations in the Northwest Atlantic. *Science* **2003**, *299* (5605), 389–392. https://doi.org/10.1126/science.1079777.

(2) Myers, R. A.; Worm, B. Rapid Worldwide Depletion of Predatory Fish Communities. *Nature* **2003**, *423* (6937), 280–283. https://doi.org/10.1038/nature01610.

(3) Ferretti, F.; Curnick, D.; Liu, K.; Romanov, E. V.; Block, B. A. Shark Baselines and the Conservation Role of Remote Coral Reef Ecosystems. *Science Advances* **2018**, *4* (3), eaaq0333. https://doi.org/10.1126/sciadv.aaq0333.

(4) Dulvy, N. K.; Pacoureau, N.; Rigby, C. L.; Pollom, R. A.; Jabado, R. W.; Ebert, D. A.; Finucci, B.; Pollock, C. M.; Cheok, J.; Derrick, D. H.; Herman, K. B.; Sherman, C. S.; VanderWright, W. J.; Lawson, J. M.; Walls, R. H. L.; Carlson, J. K.; Charvet, P.; Bineesh, K. K.; Fernando, D.; Ralph, G. M.; Matsushiba, J. H.; Hilton-Taylor, C.; Fordham, S. V.; Simpfendorfer, C. A. Overfishing Drives over One-Third of All Sharks and Rays toward a Global Extinction Crisis. *Current Biology* **2021**. https://doi.org/10.1016/j.cub.2021.08.062.

(5) Heithaus, M. R.; Frid, A.; Wirsing, A. J.; Worm, B. Predicting Ecological Consequences of Marine Top Predator Declines. *Trends in Ecology & Evolution* **2008**, *23* (4), 202–210. https://doi.org/10.1016/j.tree.2008.01.003.

(6) Ferretti, F.; Worm, B.; Britten, G. L.; Heithaus, M. R.; Lotze, H. K. Patterns and Ecosystem Consequences of Shark Declines in the Ocean. *Ecology Letters* **2010**, *13* (8), 1055–1071. https://doi.org/10.1111/j.1461-0248.2010.01489.x.

(7) Pimiento, C.; Leprieur, F.; Silvestro, D.; Lefcheck, J. S.; Albouy, C.; Rasher, D. B.; Davis, M.; Svenning, J.-C.; Griffin, J. N. Functional Diversity of Marine Megafauna in the Anthropocene. *Science Advances* **2020**, *6* (16), eaay7650. https://doi.org/10.1126/sciadv.aay7650.

(8) Pacoureau, N.; Rigby, C. L.; Kyne, P. M.; Sherley, R. B.; Winker, H.; Carlson, J. K.; Fordham, S. V.; Barreto, R.; Fernando, D.; Francis, M. P.; Jabado, R. W.; Herman, K. B.; Liu, K.-M.; Marshall, A. D.; Pollom, R. A.; Romanov, E. V.; Simpfendorfer, C. A.; Yin, J. S.; Kindsvater, H. K.; Dulvy, N. K. Half a Century of Global Decline in Oceanic Sharks and Rays. *Nature* **2021**, *589* (7843), 567–571. https://doi.org/10.1038/s41586-020-03173-9.

(9) Davenport, D.; Butcher, P.; Andreotti, S.; Matthee, C.; Jones, A.; Ovenden, J. Effective Number of White Shark (Carcharodon Carcharias, Linnaeus) Breeders Is Stable over Four Successive Years in the Population Adjacent to Eastern Australia and New Zealand. *Ecology and Evolution* **2021**, *11* (1), 186–198. https://doi.org/10.1002/ece3.7007.

(10) Moro, S.; Jona-Lasinio, G.; Block, B.; Micheli, F.; Leo, G. D.; Serena, F.; Bottaro, M.; Scacco, U.; Ferretti, F. Abundance and Distribution of the White Shark in the Mediterranean Sea. *Fish and Fisheries* **2020**, *21* (2), 338–349. https://doi.org/10.1111/faf.12432.

(11) Huveneers, C.; Apps, K.; Becerril-García, E. E.; Bruce, B.; Butcher, P. A.; Carlisle, A. B.; Chapple, T. K.; Christiansen, H. M.; Cliff, G.; Curtis, T. H.; Daly-Engel, T. S.; Dewar, H.; Dicken, M. L.; Domeier, M. L.; Duffy, C. A. J.; Ford, R.; Francis, M. P.; French, G. C. A.; Galván-Magaña, F.; García-Rodríguez, E.; Gennari, E.; Graham, B.; Hayden, B.; Hoyos-Padilla, E. M.; Hussey, N. E.; Jewell, O. J. D.; Jorgensen, S. J.; Kock, A. A.; Lowe, C. G.; Lyons, K.; Meyer, L.; Oelofse, G.; Oñate-González, E. C.; Oosthuizen, H.; O'Sullivan, J. B.; Ramm, K.; Skomal, G.; Sloan, S.; Smale, M. J.; Sosa-Nishizaki, O.; Sperone, E.; Tamburin, E.; Towner, A. V.; Wcisel, M. A.; Weng, K. C.; Werry, J. M. Future Research Directions on the "Elusive" White Shark. *Front. Mar. Sci.* **2018**, *5*. https://doi.org/10.3389/fmars.2018.00455.

(12) Le Croizier, G.; Lorrain, A.; Sonke, J. E.; Hoyos-Padilla, M.; Galván-Magaña, F.; Santana-Morales, O.; Aquino-Baleyto, M.; Becerril-García, E.; Muntaner López, G.; Block, B.; Carlisle, A.; Jorgensen, S.; Besnard, L.; Jung, A.; Schaal, G.; Point, D. The Twilight Zone as a Major Foraging Habitat and Mercury Source for the Great White Shark. *Environmental Science & Technology* **2020**. https://doi.org/10.1021/acs.est.0c05621.

(13) Jorgensen, S. J.; Reeb, C. A.; Chapple, T. K.; Anderson, S.; Perle, C.; Van Sommeran, S. R.; Fritz-Cope, C.; Brown, A. C.; Klimley, A. P.; Block, B. A. Philopatry and Migration of Pacific White Sharks. *Proceedings of the Royal Society B: Biological Sciences* **2010**, *277* (1682), 679–688. https://doi.org/10.1098/rspb.2009.1155.

(14) Blower, D. C.; Pandolfi, J. M.; Bruce, B. D.; Gomez-Cabrera, M. del C.; Ovenden, J. R. Population Genetics of Australian White Sharks Reveals Fine-Scale Spatial Structure, Transoceanic Dispersal Events and Low Effective Population Sizes. *Marine Ecology Progress Series* **2012**, *455*, 229–244. https://doi.org/10.3354/meps09659.

(15) Bradford, R.; Patterson, T. A.; Rogers, P. J.; McAuley, R.; Mountford, S.; Huveneers, C.; Robbins, R.; Fox, A.; Bruce, B. D. Evidence of Diverse Movement Strategies and Habitat Use by White Sharks, Carcharodon Carcharias, off Southern Australia. *Mar Biol* **2020**, *167* (7), 96. https://doi.org/10.1007/s00227-020-03712-y.

(16) Bruce, B. D.; Stevens, J. D.; Malcolm, H. Movements and Swimming Behaviour of White Sharks (Carcharodon Carcharias) in Australian Waters | Bycatch Management Information System (BMIS). *http://link.springer.com/article/10.1007/s00227-006-0325-1* **2006**. https://doi.org/10.1007/s00227-006-0325-1.

(17) Meyer, L.; Pethybridge, H.; Beckmann, C.; Bruce, B.; Huveneers, C. The Impact of Wildlife Tourism on the Foraging Ecology and Nutritional Condition of an Apex Predator. *Tourism Management* **2019**, *75*, 206–215. https://doi.org/10.1016/j.tourman.2019.04.025.

(18) Spaet, J. L. Y.; Patterson, T. A.; Bradford, R. W.; Butcher, P. A. Spatiotemporal Distribution Patterns of Immature Australasian White Sharks (Carcharodon Carcharias). *Scientific Reports* **2020**, *10* (1), 10169. https://doi.org/10.1038/s41598-020-66876-z.

(19) Bruce, B. D.; Harasti, D.; Lee, K.; Gallen, C.; Bradford, R. Broad-Scale Movements of Juvenile White Sharks Carcharodon Carcharias in Eastern Australia from Acoustic and Satellite Telemetry. *Marine Ecology Progress Series* **2019**, *619*, 1–15. https://doi.org/10.3354/meps12969.

(20) Duffy, C. A.; Francis, M. P.; Manning, M. J.; Bonfil, R. Regional Population Connectivity, Oceanic Habitat, and Return Migration Revealed by Satellite Tagging of White Sharks, Carcharodon Carcharias, at New Zealand Aggregation Sites. *Global perspectives on the biology and life history of the white shark* **2012**, 301–318.

(21) Bonfil, R.; Francis, M. P.; Duffy, C.; Manning, M. J.; O'Brien, S. Large-Scale Tropical Movements and Diving Behavior of White Sharks Carcharodon Carcharias Tagged off New Zealand. *Aquatic Biology* **2010**, *8* (2), 115–123. https://doi.org/10.3354/ab00217.

(22) Grainger, R.; Peddemors, V. M.; Raubenheimer, D.; Machovsky-Capuska, G. E. Diet Composition and Nutritional Niche Breadth Variability in Juvenile White Sharks (Carcharodon Carcharias). *Front. Mar. Sci.* **2020**, *7*. https://doi.org/10.3389/fmars.2020.00422.

(23) Driscoll, C. T.; Mason, R. P.; Chan, H. M.; Jacob, D. J.; Pirrone, N. Mercury as a Global Pollutant: Sources, Pathways, and Effects. *Environ. Sci. Technol.* **2013**, *47* (10), 4967–4983. https://doi.org/10.1021/es305071v.

(24) Kidd, K.; Clayden, M.; Jardine, T. Bioaccumulation and Biomagnification of Mercury through Food Webs. In *Environmental Chemistry and Toxicology of Mercury*; John Wiley & Sons, Ltd, 2011; pp 453–499. https://doi.org/10.1002/9781118146644.ch14.

(25) McKinney, M. A.; Dean, K.; Hussey, N. E.; Cliff, G.; Wintner, S. P.; Dudley, S. F. J.; Zungu, M. P.; Fisk, A. T. Global versus Local Causes and Health Implications of High Mercury Concentrations in Sharks from the East Coast of South Africa. *Science of The Total Environment* **2016**, *541*, 176–183. https://doi.org/10.1016/j.scitotenv.2015.09.074.

(26) Ehnert-Russo, S. L.; Gelsleichter, J. Mercury Accumulation and Effects in the Brain of the Atlantic Sharpnose Shark (Rhizoprionodon Terraenovae). *Arch Environ Contam Toxicol* **2020**, *78* (2), 267–283. https://doi.org/10.1007/s00244-019-00691-0.

(27) Rodrigues, A. C. M.; Gravato, C.; Galvão, D.; Silva, V. S.; Soares, A. M. V. M.; Gonçalves, J. M. S.; Ellis, J. R.; Vieira, R. Ecophysiological Effects of Mercury Bioaccumulation and Biochemical Stress in the Deep-Water Mesopredator Etmopterus Spinax (Elasmobranchii; Etmopteridae). *Journal of Hazardous Materials* **2021**, 127245. https://doi.org/10.1016/j.jhazmat.2021.127245.

(28) Le Croizier, G.; Lorrain, A.; Sonke, J. E.; Jaquemet, S.; Schaal, G.; Renedo, M.; Besnard, L.; Cherel, Y.; Point, D. Mercury Isotopes as Tracers of Ecology and Metabolism in Two Sympatric Shark Species. *Environmental Pollution* **2020**, 114931. https://doi.org/10.1016/j.envpol.2020.114931.

(29) Krey, A.; Ostertag, S. K.; Chan, H. M. Assessment of Neurotoxic Effects of Mercury in Beluga Whales (Delphinapterus Leucas), Ringed Seals (Pusa Hispida), and Polar Bears (Ursus Maritimus) from the Canadian Arctic. *Science of The Total Environment* **2015**, *509–510*, 237–247. https://doi.org/10.1016/j.scitotenv.2014.05.134.

(30) López-Berenguer, G.; Peñalver, J.; Martínez-López, E. A Critical Review about Neurotoxic Effects in Marine Mammals of Mercury and Other Trace Elements. *Chemosphere* **2020**, *246*, 125688. https://doi.org/10.1016/j.chemosphere.2019.125688.

(31) Lee, C.-S.; Lutcavage, M. E.; Chandler, E.; Madigan, D. J.; Cerrato, R. M.; Fisher, N. S. Declining Mercury Concentrations in Bluefin Tuna Reflect Reduced Emissions to the North Atlantic Ocean. *Environ. Sci. Technol.* **2016**, *50* (23), 12825–12830. https://doi.org/10.1021/acs.est.6b04328.

(32) Bank, M. S.; Frantzen, S.; Duinker, A.; Amouroux, D.; Tessier, E.; Nedreaas, K.; Maage, A.; Nilsen, B. M. Rapid Temporal Decline of Mercury in Greenland Halibut (Reinhardtius Hippoglossoides). *Environmental Pollution* **2021**, *289*, 117843. https://doi.org/10.1016/j.envpol.2021.117843.

(33) Médieu, A.; Point, D.; Receveur, A.; Gauthier, O.; Allain, V.; Pethybridge, H.; Menkes, C. E.; Gillikin, D. P.; Revill, A. T.; Somes, C. J.; Collin, J.; Lorrain, A. Stable Mercury Concentrations of Tropical Tuna in the South Western Pacific Ocean: An 18-Year Monitoring Study. *Chemosphere* **2021**, *263*, 128024. https://doi.org/10.1016/j.chemosphere.2020.128024.

(34) Yurkowski, D. J.; Richardson, E. S.; Lunn, N. J.; Muir, D. C. G.; Johnson, A. C.; Derocher, A. E.; Ehrman, A. D.; Houde, M.; Young, B. G.; Debets, C. D.; Sciullo, L.; Thiemann, G. W.; Ferguson, S. H. Contrasting Temporal Patterns of Mercury, Niche Dynamics, and Body Fat Indices of Polar Bears and Ringed Seals in a Melting Icescape. *Environ. Sci. Technol.* **2020**, *54* (5), 2780–2789. https://doi.org/10.1021/acs.est.9b06656.

(35) Drevnick, P. E.; Lamborg, C. H.; Horgan, M. J. Increase in Mercury in Pacific Yellowfin Tuna. *Environmental Toxicology and Chemistry* **2015**, *34* (4), 931–934. https://doi.org/10.1002/etc.2883.

(36) Dietz, R.; Desforges, J.-P.; Rigét, F. F.; Aubail, A.; Garde, E.; Ambus, P.; Drimmie, R.; Heide-Jørgensen, M. P.; Sonne, C. Analysis of Narwhal Tusks Reveals Lifelong Feeding Ecology and Mercury Exposure. *Current Biology* **2021**. https://doi.org/10.1016/j.cub.2021.02.018.

(37) Vo, A.-T. E.; Bank, M. S.; Shine, J. P.; Edwards, S. V. Temporal Increase in Organic Mercury in an Endangered Pelagic Seabird Assessed by Century-Old Museum Specimens. *PNAS* **2011**, *108* (18), 7466–7471. https://doi.org/10.1073/pnas.1013865108.

(38) Schartup, A. T.; Thackray, C. P.; Qureshi, A.; Dassuncao, C.; Gillespie, K.; Hanke, A.; Sunderland, E. M. Climate Change and Overfishing Increase Neurotoxicant in Marine Predators. *Nature* **2019**, *572* (7771), 648–650. https://doi.org/10.1038/s41586-019-1468-9.

(39) Alava, J. J.; Cisneros-Montemayor, A. M.; Sumaila, U. R.; Cheung, W. W. L. Projected Amplification of Food Web Bioaccumulation of MeHg and PCBs under Climate Change in the Northeastern Pacific. *Sci Rep* **2018**, *8* (1), 13460. https://doi.org/10.1038/s41598-018-31824-5.

(40) Booth, S.; Zeller, D. Mercury, Food Webs, and Marine Mammals: Implications of Diet and Climate Change for Human Health. *Environmental Health Perspectives* **2005**, *113* (5), 521–526. https://doi.org/10.1289/ehp.7603.

(41) Peterson, S. H.; Ackerman, J. T.; Costa, D. P. Marine Foraging Ecology Influences Mercury Bioaccumulation in Deep-Diving Northern Elephant Seals. *Proceedings of the Royal Society B: Biological Sciences* **2015**, *282* (1810), 20150710. https://doi.org/10.1098/rspb.2015.0710.

(42) Blum, J. D.; Popp, B. N.; Drazen, J. C.; Anela Choy, C.; Johnson, M. W. Methylmercury Production below the Mixed Layer in the North Pacific Ocean. *Nature Geosci* **2013**, *6* (10), 879–884. https://doi.org/10.1038/ngeo1918.

(43) Renedo, M.; Amouroux, D.; Pedrero, Z.; Bustamante, P.; Cherel, Y. Identification of Sources and Bioaccumulation Pathways of MeHg in Subantarctic Penguins: A Stable Isotopic Investigation. *Sci Rep* **2018**, *8* (1), 8865. https://doi.org/10.1038/s41598-018-27079-9.

(44) Li, M.; Juang, C. A.; Ewald, J. D.; Yin, R.; Mikkelsen, B.; Krabbenhoft, D. P.; Balcom, P. H.; Dassuncao, C.; Sunderland, E. M. Selenium and Stable Mercury Isotopes Provide New Insights into

Mercury Toxicokinetics in Pilot Whales. *Science of The Total Environment* **2020**, *710*, 136325. https://doi.org/10.1016/j.scitotenv.2019.136325.

(45) Bergquist, B. A.; Blum, J. D. Mass-Dependent and -Independent Fractionation of Hg Isotopes by Photoreduction in Aquatic Systems. *Science* **2007**, *318* (5849), 417–420. https://doi.org/10.1126/science.1148050.

(46) Zheng, W.; Foucher, D.; Hintelmann, H. Mercury Isotope Fractionation during Volatilization of Hg(0) from Solution into the Gas Phase. *Journal of Analytical Atomic Spectrometry* **2007**, *22* (9), 1097–1104. https://doi.org/10.1039/B705677J.

(47) Perrot, V.; Masbou, J.; V. Pastukhov, M.; N. Epov, V.; Point, D.; Bérail, S.; R. Becker, P.; E. Sonke, J.; Amouroux, D. Natural Hg Isotopic Composition of Different Hg Compounds in Mammal Tissues as a Proxy for in Vivo Breakdown of Toxic Methylmercury. *Metallomics* **2016**, *8* (2), 170–178. https://doi.org/10.1039/C5MT00286A.

(48) Janssen, S. E.; Schaefer, J. K.; Barkay, T.; Reinfelder, J. R. Fractionation of Mercury Stable Isotopes during Microbial Methylmercury Production by Iron- and Sulfate-Reducing Bacteria. *Environ. Sci. Technol.* **2016**, *50* (15), 8077–8083. https://doi.org/10.1021/acs.est.6b00854.

(49) Chen, J.; Hintelmann, H.; Feng, X.; Dimock, B. Unusual Fractionation of Both Odd and Even Mercury Isotopes in Precipitation from Peterborough, ON, Canada. *Geochimica et Cosmochimica Acta* **2012**, *90*, 33–46. https://doi.org/10.1016/j.gca.2012.05.005.

(50) Jiskra, M.; Heimbürger-Boavida, L.-E.; Desgranges, M.-M.; Petrova, M. V.; Dufour, A.; Ferreira-Araujo, B.; Masbou, J.; Chmeleff, J.; Thyssen, M.; Point, D.; Sonke, J. E. Mercury Stable Isotopes Constrain Atmospheric Sources to the Ocean. *Nature* **2021**, *597* (7878), 678–682. https://doi.org/10.1038/s41586-021-03859-8.

(51) Tsui, M. T.-K.; Blum, J. D.; Kwon, S. Y. Review of Stable Mercury Isotopes in Ecology and Biogeochemistry. *Science of The Total Environment* **2020**, *716*, 135386. https://doi.org/10.1016/j.scitotenv.2019.135386.

(52) Le Croizier, G.; Lorrain, A.; Sonke, J. E.; Jaquemet, S.; Schaal, G.; Renedo, M.; Besnard, L.; Cherel, Y.; Point, D. Mercury Isotopes as Tracers of Ecology and Metabolism in Two Sympatric Shark Species. *Environmental Pollution* **2020**, *265*, 114931. https://doi.org/10.1016/j.envpol.2020.114931.

(53) Cransveld, A.; Amouroux, D.; Tessier, E.; Koutrakis, E.; Ozturk, A. A.; Bettoso, N.; Mieiro, C. L.; Bérail, S.; Barre, J. P. G.; Sturaro, N.; Schnitzler, J.; Das, K. Mercury Stable Isotopes Discriminate Different Populations of European Seabass and Trace Potential Hg Sources around Europe. *Environ. Sci. Technol.* **2017**, *51* (21), 12219–12228. https://doi.org/10.1021/acs.est.7b01307.

(54) Pinzone, M.; Cransveld, A.; Tessier, E.; Bérail, S.; Schnitzler, J.; Das, K.; Amouroux, D. Contamination Levels and Habitat Use Influence Hg Accumulation and Stable Isotope Ratios in the European Seabass Dicentrarchus Labrax. *Environmental Pollution* **2021**, *281*, 117008. https://doi.org/10.1016/j.envpol.2021.117008.

(55) Meyer, L.; Fox, A.; Huveneers, C. Simple Biopsy Modification to Collect Muscle Samples from Free-Swimming Sharks. *Biological Conservation* **2018**, *228*, 142–147. https://doi.org/10.1016/j.biocon.2018.10.024.

(56) Tate, R. D.; Kelaher, B. P.; Brand, C. P.; Cullis, B. R.; Gallen, C. R.; Smith, S. D. A.; Butcher, P. A. The Effectiveness of Shark-Management-Alert-in-Real-Time (SMART) Drumlines as a Tool for Catching White Sharks, *Carcharodon Carcharias* , off Coastal New South Wales, Australia. *Fish Manag Ecol* **2021**, fme.12489. https://doi.org/10.1111/fme.12489.

(57) Tate, R. D.; Cullis, B. R.; Smith, S. D. A.; Kelaher, B. P.; Brand, C. P.; Gallen, C. R.; Mandelman, J. W.; Butcher, P. A. The Acute Physiological Status of White Sharks (Carcharodon Carcharias) Exhibits Minimal Variation after Capture on SMART Drumlines. *Conservation Physiology* **2019**, *7* (1), coz042. https://doi.org/10.1093/conphys/coz042.

(58) May, C.; Meyer, L.; Whitmarsh, S.; Huveneers, C. Eyes on the Size: Accuracy of Visual Length Estimates of White Sharks, Carcharodon Carcharias. *Royal Society Open Science 6* (5), 190456. https://doi.org/10.1098/rsos.190456.

(59) Matulik, A. G.; Kerstetter, D. W.; Hammerschlag, N.; Divoll, T.; Hammerschmidt, C. R.; Evers, D. C. Bioaccumulation and Biomagnification of Mercury and Methylmercury in Four Sympatric Coastal Sharks in a Protected Subtropical Lagoon. *Marine Pollution Bulletin* **2017**, *116* (1), 357–364. https://doi.org/10.1016/j.marpolbul.2017.01.033.

(60) Pethybridge, H.; Cossa, D.; Butler, E. C. V. Mercury in 16 Demersal Sharks from Southeast Australia: Biotic and Abiotic Sources of Variation and Consumer Health Implications. *Marine Environmental Research* **2010**, *69* (1), 18–26. https://doi.org/10.1016/j.marenvres.2009.07.006.

(61) de Carvalho, G. G. A.; Degaspari, I. A. M.; Branco, V.; Canário, J.; de Amorim, A. F.; Kennedy, V. H.; Ferreira, J. R. Assessment of Total and Organic Mercury Levels in Blue Sharks (Prionace Glauca) from the South and Southeastern Brazilian Coast. *Biol Trace Elem Res* **2014**, *159* (1), 128–134. https://doi.org/10.1007/s12011-014-9995-6.

(62) Bosch, A. C.; O'Neill, B.; Sigge, G. O.; Kerwath, S. E.; Hoffman, L. C. Heavy Metal Accumulation and Toxicity in Smoothhound (Mustelus Mustelus) Shark from Langebaan Lagoon, South Africa. *Food Chemistry* **2016**, *190*, 871–878. https://doi.org/10.1016/j.foodchem.2015.06.034.

(63) Nalluri, D.; Baumann, Z.; Abercrombie, D. L.; Chapman, D. D.; Hammerschmidt, C. R.; Fisher, N. S. Methylmercury in Dried Shark Fins and Shark Fin Soup from American Restaurants. *Science of The Total Environment* **2014**, *496*, 644–648. https://doi.org/10.1016/j.scitotenv.2014.04.107.

(64) Besnard, L.; Le Croizier, G.; Galván-Magaña, F.; Point, D.; Kraffe, E.; Ketchum, J.; Martinez Rincon, R. O.; Schaal, G. Foraging Depth Depicts Resource Partitioning and Contamination Level in a Pelagic Shark Assemblage: Insights from Mercury Stable Isotopes. *Environmental Pollution* **2021**, 117066. https://doi.org/10.1016/j.envpol.2021.117066.

(65) Masbou, J.; Point, D.; Sonke, J. E. Application of a Selective Extraction Method for Methylmercury Compound Specific Stable Isotope Analysis (MeHg-CSIA) in Biological Materials. *J. Anal. At. Spectrom.* **2013**, *28* (10), 1620–1628. https://doi.org/10.1039/C3JA50185J.

(66) Jiskra, M.; G. Wiederhold, J.; Skyllberg, U.; Kronberg, R.-M.; Kretzschmar, R. Source Tracing of Natural Organic Matter Bound Mercury in Boreal Forest Runoff with Mercury Stable Isotopes. *Environmental Science: Processes & Impacts* **2017**, *19* (10), 1235–1248. https://doi.org/10.1039/C7EM00245A.

(67) Lepak, R. F.; Janssen, S. E.; Yin, R.; Krabbenhoft, D. P.; Ogorek, J. M.; DeWild, J. F.; Tate, M. T.; Holsen, T. M.; Hurley, J. P. Factors Affecting Mercury Stable Isotopic Distribution in Piscivorous Fish of the Laurentian Great Lakes. *Environ. Sci. Technol.* **2018**, *52* (5), 2768–2776. https://doi.org/10.1021/acs.est.7b06120.

(68) Masbou, J.; Sonke, J. E.; Amouroux, D.; Guillou, G.; Becker, P. R.; Point, D. Hg-Stable Isotope Variations in Marine Top Predators of the Western Arctic Ocean. *ACS Earth Space Chem.* **2018**. https://doi.org/10.1021/acsearthspacechem.8b00017.

(69) Enrico, M.; Roux, G. L.; Marusczak, N.; Heimbürger, L.-E.; Claustres, A.; Fu, X.; Sun, R.; Sonke, J. E. Atmospheric Mercury Transfer to Peat Bogs Dominated by Gaseous Elemental Mercury Dry Deposition. *Environ. Sci. Technol.* **2016**, *50* (5), 2405–2412. https://doi.org/10.1021/acs.est.5b06058.

(70) Obrist, D.; Agnan, Y.; Jiskra, M.; Olson, C. L.; Colegrove, D. P.; Hueber, J.; Moore, C. W.; Sonke, J. E.; Helmig, D. Tundra Uptake of Atmospheric Elemental Mercury Drives Arctic Mercury Pollution. *Nature* **2017**, *547* (7662), 201–204. https://doi.org/10.1038/nature22997.

(71) Meng, M.; Sun, R.; Liu, H.; Yu, B.; Yin, Y.; Hu, L.; Chen, J.; Shi, J.; Jiang, G. Mercury Isotope Variations within the Marine Food Web of Chinese Bohai Sea: Implications for Mercury Sources and Biogeochemical Cycling. *Journal of Hazardous Materials* **2020**, *384*, 121379. https://doi.org/10.1016/j.jhazmat.2019.121379.

(72) Motta, L. C.; Blum, J. D.; Johnson, M. W.; Umhau, B. P.; Popp, B. N.; Washburn, S. J.; Drazen, J. C.; Benitez-Nelson, C. R.; Hannides, C. C. S.; Close, H. G.; Lamborg, C. H. Mercury Cycling in the North Pacific Subtropical Gyre as Revealed by Mercury Stable Isotope Ratios. *Global Biogeochemical Cycles* **2019**, *33* (6), 777–794. https://doi.org/10.1029/2018GB006057.

(73) Le Croizier, G.; Lorrain, A.; Sonke, J. E.; Hoyos-Padilla, E. M.; Galván-Magaña, F.; Santana-Morales, O.; Aquino-Baleytó, M.; Becerril-García, E. E.; Muntaner-López, G.; Ketchum, J.; Block, B.; Carlisle, A.; Jorgensen, S. J.; Besnard, L.; Jung, A.; Schaal, G.; Point, D. The Twilight Zone as a Major Foraging Habitat and Mercury Source for the Great White Shark. *Environ. Sci. Technol.* **2020**. https://doi.org/10.1021/acs.est.0c05621.

(74) Kwon, S. Y.; Blum, J. D.; Carvan, M. J.; Basu, N.; Head, J. A.; Madenjian, C. P.; David, S. R. Absence of Fractionation of Mercury Isotopes during Trophic Transfer of Methylmercury to Freshwater Fish in Captivity. *Environ. Sci. Technol.* **2012**, *46* (14), 7527–7534. https://doi.org/10.1021/es300794q.

(75) Sackett, D. K.; Drazen, J. C.; Popp, B. N.; Choy, C. A.; Blum, J. D.; Johnson, M. W. Carbon, Nitrogen, and Mercury Isotope Evidence for the Biogeochemical History of Mercury in Hawaiian Marine Bottomfish. *Environ. Sci. Technol.* **2017**, *51* (23), 13976–13984. https://doi.org/10.1021/acs.est.7b04893.

(76) Senn, D. B.; Chesney, E. J.; Blum, J. D.; Bank, M. S.; Maage, A.; Shine, J. P. Stable Isotope (N, C, Hg) Study of Methylmercury Sources and Trophic Transfer in the Northern Gulf of Mexico. *Environ. Sci. Technol.* **2010**, *44* (5), 1630–1637. https://doi.org/10.1021/es902361j.

(77) Perrot, V.; Landing, W. M.; Grubbs, R. D.; Salters, V. J. M. Mercury Bioaccumulation in Tilefish from the Northeastern Gulf of Mexico 2 years after the Deepwater Horizon Oil Spill: Insights from Hg, C, N and S Stable Isotopes. *Science of The Total Environment* **2019**, *666*, 828–838. https://doi.org/10.1016/j.scitotenv.2019.02.295.

(78) Sun, L.; Chen, W.; Yuan, D.; Zhou, L.; Lu, C.; Zheng, Y. Distribution and Transformation of Mercury in Subtropical Wild-Caught Seafood from the Southern Taiwan Strait. *Biol Trace Elem Res* **2021**. https://doi.org/10.1007/s12011-021-02695-1.

(79) Motta, L. C.; Blum, J. D.; Popp, B. N.; Drazen, J. C.; Close, H. G. Mercury Stable Isotopes in Flying Fish as a Monitor of Photochemical Degradation of Methylmercury in the Atlantic and Pacific Oceans. *Marine Chemistry* **2020**, *223*, 103790. https://doi.org/10.1016/j.marchem.2020.103790.

(80) He, X.; Pan, D.; Bai, Y.; Wang, T.; Chen, C.-T. A.; Zhu, Q.; Hao, Z.; Gong, F. Recent Changes of Global Ocean Transparency Observed by SeaWiFS. *Continental Shelf Research* **2017**, *143*, 159–166. https://doi.org/10.1016/j.csr.2016.09.011.

(81) Lee, K. A.; Butcher, P. A.; Harcourt, R. G.; Patterson, T. A.; Peddemors, V. M.; Roughan, M.; Harasti, D.; Smoothey, A. F.; Bradford, R. W. Oceanographic Conditions Associated with White Shark (Carcharodon Carcharias) Habitat Use along Eastern Australia. *Marine Ecology Progress Series* **2021**, *659*, 143–159. https://doi.org/10.3354/meps13572.

(82) Poulin, B. A.; Janssen, S. E.; Rosera, T. J.; Krabbenhoft, D. P.; Eagles-Smith, C. A.; Ackerman, J. T.; Stewart, A. R.; Kim, E.; Baumann, Z.; Kim, J.-H.; Manceau, A. Isotope Fractionation from In Vivo Methylmercury Detoxification in Waterbirds. *ACS Earth Space Chem.* **2021**. https://doi.org/10.1021/acsearthspacechem.1c00051.

(83) Renedo, M.; Pedrero, Z.; Amouroux, D.; Cherel, Y.; Bustamante, P. Mercury Isotopes of Key Tissues Document Mercury Metabolic Processes in Seabirds. *Chemosphere* **2021**, *263*, 127777. https://doi.org/10.1016/j.chemosphere.2020.127777.

(84) Hussey, N. E.; McCann, H. M.; Cliff, G.; Dudley, S. F.; Wintner, S. P.; Fisk, A. T. Size-Based Analysis of Diet and Trophic Position of the White Shark (Carcharodon Carcharias) in South African Waters. *Global Perspectives on the Biology and Life History of the White Shark'.(Ed. ML Domeier.) pp* **2012**, 27–49.

(85) Bolea-Fernández, E.; Rua-Ibarz, A.; Krupp, E.; Feldmann, J.; Vanhaecke, F. High-Precision Isotopic Analysis Sheds New Light on Mercury Metabolism in Long-Finned Pilot Whales (Globicephala Melas). *Scientific Reports* **2019**, *9*. https://doi.org/10.1038/s41598-019-43825-z.

(86) Spaet, J. L. Y.; Manica, A.; Brand, C. P.; Gallen, C.; Butcher, P. A. Environmental Conditions Are Poor Predictors of Immature White Shark Carcharodon Carcharias Occurrences on Coastal Beaches of Eastern Australia. *Marine Ecology Progress Series* **2020**, *653*, 167–179. https://doi.org/10.3354/meps13488.

(87) Francis, M. P.; Duffy, C.; Lyon, W.; Francis, M. P.; Duffy, C.; Lyon, W. Spatial and Temporal Habitat Use by White Sharks (Carcharodon Carcharias) at an Aggregation Site in Southern New Zealand. *Mar. Freshwater Res.* **2015**, *66* (10), 900–918. https://doi.org/10.1071/MF14186.

(88) Wang, W.-X.; Wong, R. S. K. Bioaccumulation Kinetics and Exposure Pathways of Inorganic Mercury and Methylmercury in a Marine Fish, the Sweetlips Plectorhinchus Gibbosus. *Marine Ecology Progress Series* **2003**, *261*, 257–268. https://doi.org/10.3354/meps261257.

(89) Manceau, A.; Bourdineaud, J.-P.; Oliveira, R. B.; Sarrazin, S. L. F.; Krabbenhoft, D. P.; Eagles-Smith, C. A.; Ackerman, J. T.; Stewart, A. R.; Ward-Deitrich, C.; del Castillo Busto, M. E.; Goenaga-Infante, H.; Wack, A.; Retegan, M.; Detlefs, B.; Glatzel, P.; Bustamante, P.; Nagy, K. L.; Poulin, B. A. Demethylation of Methylmercury in Bird, Fish, and Earthworm. *Environ. Sci. Technol.* **2021**, *55* (3), 1527–1534. https://doi.org/10.1021/acs.est.0c04948.

(90) Gilbert, J. M.; Reichelt-Brushett, A. J.; Butcher, P. A.; McGrath, S. P.; Peddemors, V. M.; Bowling, A. C.; Christidis, L. Metal and Metalloid Concentrations in the Tissues of Dusky Carcharhinus Obscurus, Sandbar C. Plumbeus and White Carcharodon Carcharias Sharks from South-Eastern Australian Waters, and the Implications for Human Consumption. *Marine Pollution Bulletin* **2015**, *92* (1), 186–194. https://doi.org/10.1016/j.marpolbul.2014.12.037.

(91) Kemper, C.; Gibbs, P.; Obendorf, D.; Marvanek, S.; Lenghaus, C. A Review of Heavy Metal and Organochlorine Levels in Marine Mammals in Australia. *Science of The Total Environment* **1994**, *154* (2), 129–139. https://doi.org/10.1016/0048-9697(94)90083-3.

(92) Pethybridge, H.; Daley, R.; Virtue, P.; Butler, E. C. V.; Cossa, D.; Nichols, P. D.; Pethybridge, H.; Daley, R.; Virtue, P.; Butler, E. C. V.; Cossa, D.; Nichols, P. D. Lipid and Mercury Profiles of 61 Mid-trophic Species Collected off South-eastern Australia. *Mar. Freshwater Res.* **2010**, *61* (10), 1092–1108. https://doi.org/10.1071/MF09237.

(93) Ohkouchi, N.; Chikaraishi, Y.; Close, H. G.; Fry, B.; Larsen, T.; Madigan, D. J.; McCarthy, M. D.; McMahon, K. W.; Nagata, T.; Naito, Y. I.; Ogawa, N. O.; Popp, B. N.; Steffan, S.; Takano, Y.; Tayasu, I.; Wyatt, A. S. J.; Yamaguchi, Y. T.; Yokoyama, Y. Advances in the Application of Amino Acid Nitrogen Isotopic Analysis in Ecological and Biogeochemical Studies. *Organic Geochemistry* **2017**, *113*, 150–174. https://doi.org/10.1016/j.orggeochem.2017.07.009.

Figure 1: Map of the spatial distribution of white sharks from the north-eastern Pacific (NEP), eastern Australasian (EA) and south-western Australasian (SWA) populations. Sample collection sites are figured (*).

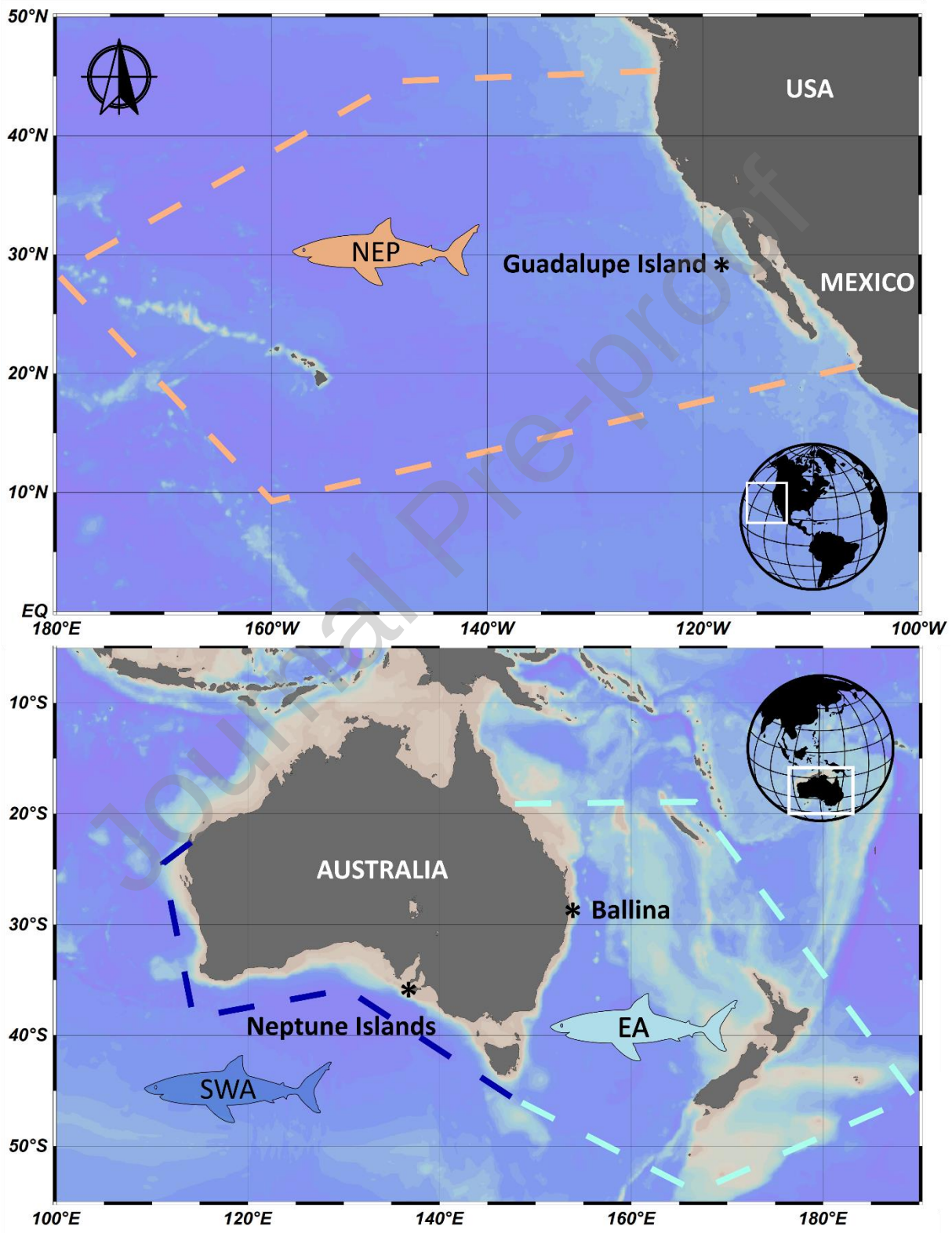

Figure 2: Raw data points, boxplots and data distribution of A) Δ^{200}Hg, B) Δ^{199}Hg and C) δ^{202}Hg values in the muscle of different white shark populations: the north-eastern Pacific (NEP), eastern Australasian (EA) and south-western Australasian (SWA) populations. Different letters indicate significant differences between populations (ANOVAs; $p < 0.05$).

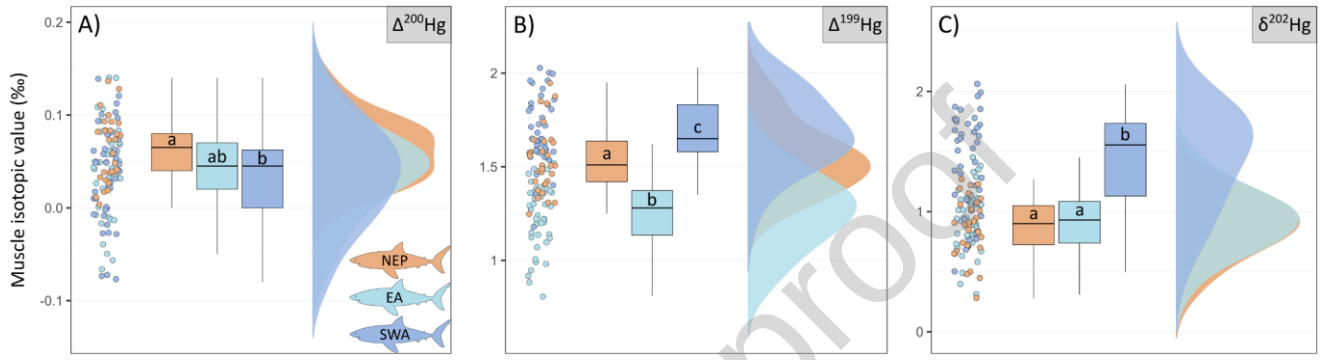

Figure 3: Relationships between A) Δ^{199}Hg, B) δ^{202}Hg and C) Δ^{200}Hg values and body length in the eastern Australasian (EA) and south-western Australasian (SWA) populations. Data fits a linear regression in A) R^2=0.40, p<0.001; B) R^2=0.49, p<0.001 and C) R^2=0.26, p<0.01.

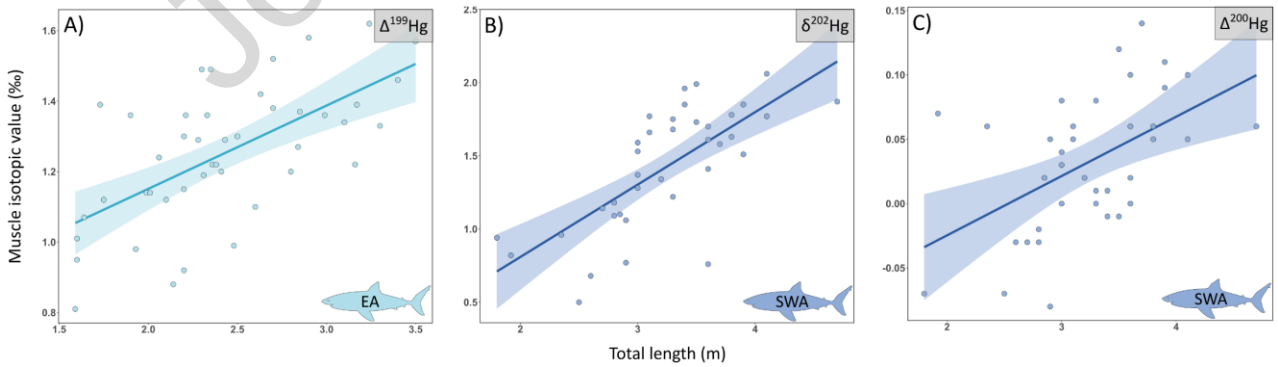

Figure 4: Relationships between log-transformed Hg concentration and total length (m) in the muscle of different white shark populations: the north-eastern Pacific (NEP), eastern

Australasian (EA) and south-western Australasian (SWA) populations. Data fits a linear regression in the EA (R^2=0.41, p<0.001) and SWA (R^2=0.50, p<0.001) populations, but not in the NEP population (p>0.05).

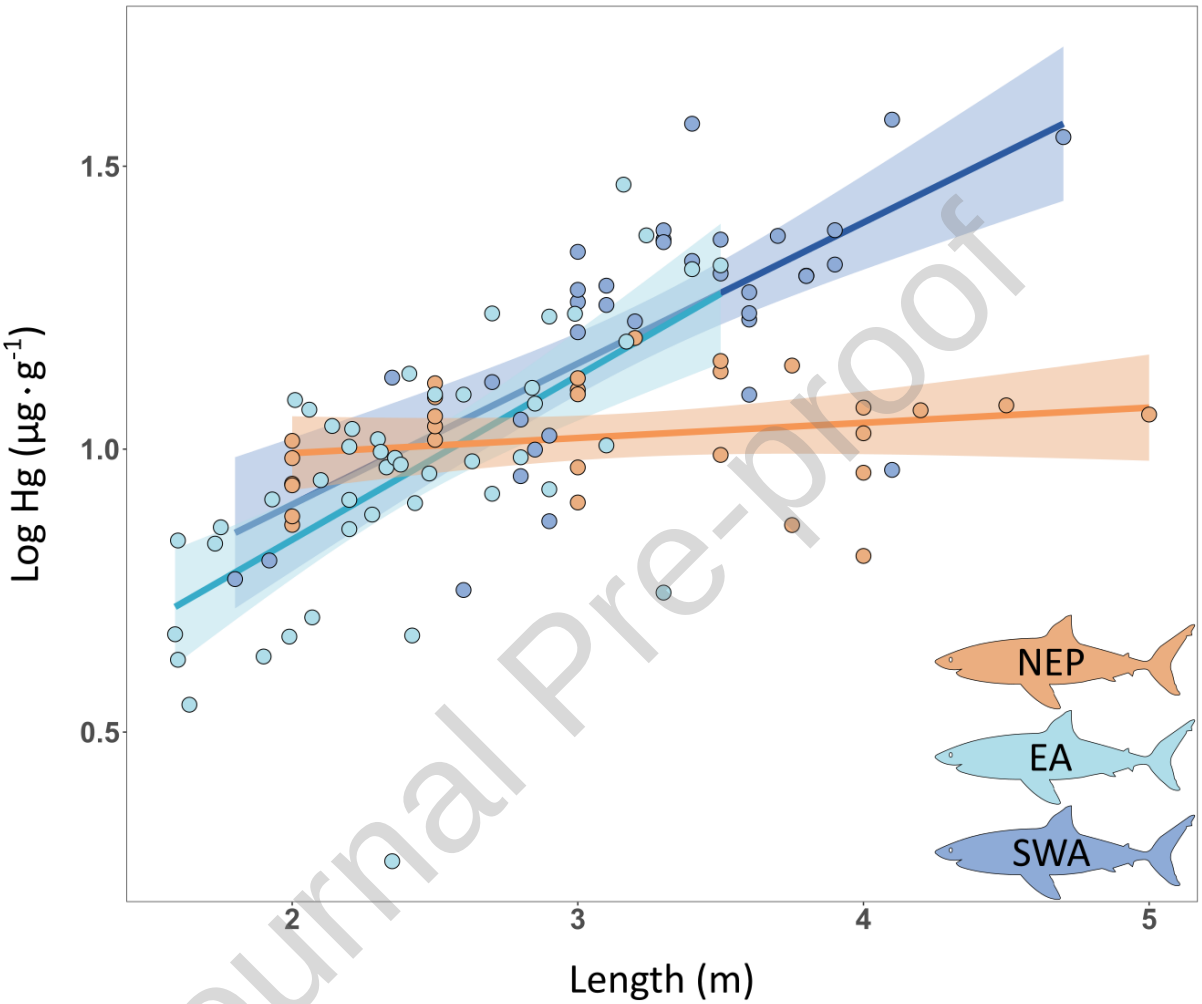

Table 1: Summary of Hg analyses (mean ± standard deviation) carried out in white shark muscle. Shark length is indicated as mean (range). Habitat characteristics are reported according to previous studies [46,47,53,54].

Population	n	Total length (m)	Maturity stage	THg ($\mu g \cdot g^{-1}$)	$\delta^{202}Hg$ (‰)	$\Delta^{199}Hg$ (‰)	$\Delta^{200}Hg$ (‰)	Vertical habitat	Horizontal habitat	Secchi depth
North-eastern Pacific (NEP)	30	3.1 (2.0-5.0)	Juvenile to adult	10.58 ± 2.64	0.88 ± 0.25	1.54 ± 0.18	0.06 ± 0.03	Epi to mesopelagic	Offshore	50
Eastern Australasian (EA)	44	2.4 (1.6-3.5)	Juvenile to subadult	10.50 ± 5.51	0.92 ± 0.25	1.25 ± 0.19	0.04 ± 0.05	Epipelagic	Continental shelf	30
South-western Australasian (SWA)	40	3.2 (1.8-4.7)	Juvenile to adult	18.31 ± 8.08	1.43 ± 0.40	1.69 ± 0.19	0.03 ± 0.05	Epipelagic	Continental shelf	30

Graphical abstract

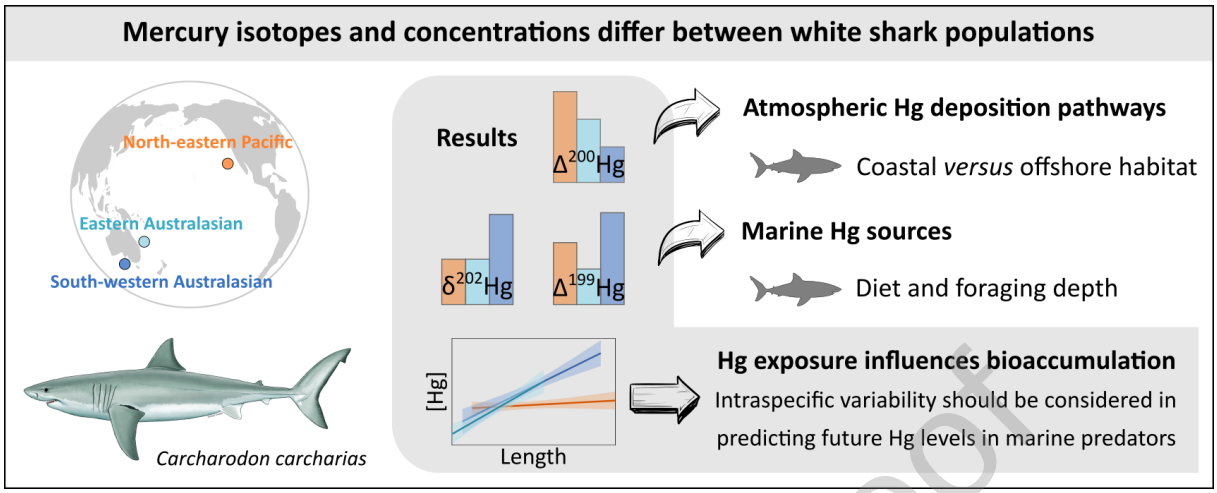

CRediT authorship contribution statement

Gaël Le Croizier: Conceptualization, Methodology, Formal analysis, Writing - Original Draft, Writing - Review & Editing. **Jeroen Sonke**: Formal analysis, Resources, Writing - Review & Editing, Supervision, Funding acquisition. **Anne Lorrain** Resources, Writing - Review & Editing, Supervision, Funding acquisition. **Marina Renedo**: Formal analysis, Writing - Review & Editing. **Mauricio Hoyos-Padilla**: Investigation, Resources, Writing - Review & Editing, Funding acquisition. **Omar Santana-Morales**: Investigation, Resources, Writing - Review & Editing, Funding acquisition. **Lauren Meyer**: Investigation, Resources, Writing - Review & Editing, Funding acquisition. **Charlie Huveneers**: Investigation, Resources, Writing - Review & Editing, Funding acquisition. **Paul Butcher**: Investigation, Resources, Writing - Review & Editing, Funding acquisition. **Felipe Amezcua-Martinez**: Writing - Review & Editing. **David Point**: Resources, Writing - Review & Editing, Supervision, Funding acquisition.

Declaration of interests

☒ The authors declare that they have no known competing financial interests or personal relationships that could have appeared to influence the work reported in this paper.

☐The authors declare the following financial interests/personal relationships which may be considered as potential competing interests:

Highlights

- Mercury (Hg) isotopes were analyzed in three white shark populations
- Δ^{200}Hg values showed different atmospheric Hg deposition pathways across habitats
- Δ^{199}Hg and δ^{202}Hg values indicated population variations in marine Hg exposure
- Hg concentrations in adult sharks differed by a factor of three between populations
- Hg contamination in ocean predators may not vary uniformly under global change